IAC-22-A1.5.70998

Target Effects vs. Non-Target Effects in Estimating the Carcinogenics Risk due to Galactic Cosmic Rays in Exploratory Space Missions.

Aboma N. Guracho [a], Lidia Strigari[b], Alessandro Bartoloni[c*]

[a] *Roma Division, Italian Institute for Nuclear Physics, Ple Aldo Moro 2, 00185, Roma, Italy,* aboma.guracho@roma1.infn.it
[b] *Department of Medical Physics , IRCCS University Hospital of Bologna, Via Massarenti 9, 40138 , Bologna, Italy,* lidia.strigari@aosp.bo.it
[c] *Roma Division, Italian Institute for Nuclear Physics, Ple Aldo Moro 2, 00185, Roma, Italy,* alessandro.bartoloni@roma1.infn.it

* Corresponding Author

Abstract

Space radiobiology is an interdisciplinary science that examines the biological effects of ionizing radiation on humans involved in aerospace missions. The knowledge of the risk assessment of the health hazard related to human space exploration is crucial to reducing damages induced to astronauts from galactic cosmic rays and sun-generated radiation. Galactic Cosmic Rays (GCRs) have been identified as one of the primary sources of radiation exposure in space. In this context, an accurate characterization of the possible risk of carcinogenesis induced by exposure to GCRs particles is a significant concern for human exploratory space missions. In this talk, the tumour prevalence is used to investigate the effects of Non-Target Effects (NTEs) in predictions of chronic GCR exposure risk. The NTE model led to a predicted risk 2-fold higher com-pared to a targeted effects model. Therefore, it is nowadays accepted that the detrimental effects of ionizing radiation are not restricted only in the irradiated cells but also to non-irradiated bystanders or even distant cells manifesting various biological effects. In this talk, an extensive study will be presented about the risk increase due to the Non-Target Effects that the GCRs radiation will imply when added to the Target one. Status of the art results will be summarized, recent observations and theoretical framework present-ed, and some new hints derived from the data collected from the AMS02 detector. Finally, the possible future development will be highlighted about the possibility of an accurate estimate of the tumour prevalence function for different exposure exploratory space mission scenarios.

Keywords: Human Space exploration, Space Radiation, Space Radiobiology, Radiation Dose-Effects Model, Cancer Risk, Astroparticle Experiments

Nomenclature

$^{1}_{1}H$	Hydrogen
$^{4}_{2}He$	Helium
$^{14}_{28}Si$	Silicon
$^{20}_{10}Ne$	Neon
$^{22}_{48}Ti$	Titanium
$^{43}_{93}Nb$	Niobium
$^{56}_{26}Fe$	Iron
$^{57}_{139}La$	Lantanio

Acronyms/Abbreviations

BE	Bystander Effects
BLEO	Beyond Low Earth Orbit
CP	Charged Particle
CSP	Cell Survival Function
DEM	Dose-Effects Model
DER	Dose-Effects Relationship
GCR	Galactic Cosmic Ray
HGT	Harderian Gland Tumour
IR	Ionising Radiation
LEO	Low Earth Orbit
LET	Linear Energy Transfer
NTE	Non-Target Effects
RBE	Relative Biological Effectiveness
TE	Target Effects
TP	Tumour Prevalence

1. Introduction

1.1 Space Radiation induced health risk

The health risks from Galactic Cosmic Rays (GCRs) exposure to astronauts include cancer [1], central nervous system effects [2, 4], cataracts, circulatory diseases, and acute radiation syndromes [5-9].

Cancer and cataracts are the main concern for space missions in Low Earth Orbit (LEO), while for long-term space missions in Beyond Low Earth Orbit (BLEO), outside the protection of the Earth's magnetic field

cancer risks are predicted to exceed acceptable risk levels, and non-cancer risks are of concern [7, 8] for the higher doses at the organ. Annual organ absorbed doses and doses equivalents due to GCR vary over the solar cycle between 0.1 and 0.2 Gy/y and 0.3 and 0.6 Sv/yr, respectively for average spacecraft shielding thicknesses [10, 11]. Protons dominate absorbed doses, while heavy ions, low energy protons and helium particles, and neutrons make important contributions to dose equivalent because of their large quality factors. The high energies of GCRs limit practical shielding amounts from providing significant attenuation [11]. The exploration of Mars will require missions of 900 days or longer with more than one year in deep space where exposures to all energies of GCRs are unavoidable and doses only modestly decreased by radiation shielding.

1.2 Carcinogenic Risk

Extensive studies of the life-shortening and carcinogenic effects of high-Linear Energy Transfer (LET) radiation have been reported over the years. A few examples of these are reported about the carcinogenic potential of neutrons [12 - 15], also review by Sinclair [16], and early workers on high-Z, high-LET charged particle (CP) from different laboratories [18].

There are several uncertainties in estimating space radiation cancer risks, including radiation quality and dose-rate effects, the transfer of epidemiology data between populations, and statistical and bias errors in epidemiology data. Of these uncertainties, estimating radiation quality effects due to the lack of human data for the heavy ions and other high LET radiations that occur in space, is the largest [19].

Both quantitative and qualitative differences between high and low LET cancer risks are possible with the later suggesting inadequacies in the use of relative biological effectiveness (RBE) factors as a basis for risk estimates.

Experimental studies of tumour induction in mice and surrogate cancer risk endpoints in cell culture models are used to estimate radiation quality factors and their uncertainties1. In studies of tumour induction with heavy ions, HGT in female B6CF1 mice has been the only study that has used a sufficient number of particle types (>4) and low doses (<0.2 Gy) to make a detailed study of radiation quality effects [20 - 23].

Energy deposition by particles in biomolecules, cells, and tissues depends on several physical aspects of particle tracks including a core of very high energy deposition events near the particles path, and a so-called penumbra of energetic electrons denoted as δ-rays liberated in ionization by primary particles and electrons, which may extend for 100's of microns from the particles path. Other considerations are the varying ranges or cells traversed in tissue of particles of similar LETs but different charge number or kinetic energy, and the effects of projectile and target fragmentation caused by nuclear interactions. Both theoretical analysis and experimental studies suggest that biological effectiveness is dependent on particle energy and charge number and not LET alone due to the above noted physical characteristics. It is interest to understand NTE including bystander effects (BEs) in neighbour cells of cells directly hit by radiation tracks how could impact our understanding of cancer risks from GCR, which are comprised of high-energy protons and heavy ions [24-27].

1.3 Bystander Effects and Space Radiation

Non-Targeted Effects (NTEs) include BEs where cells traversed by heavy ions transmit oncogenic signals to nearby cells, and genomic instability in the progeny of irradiated cells. Analysis of the Harderian gland studies, [23, 22-27] and experiments for chromosomal aberrations at low dose [28,29] suggests a model based on Non-Targeted Effects (NTE) is favoured over a Targeted Effects (TE) model, where the later assumes a linear dose response model consistent with DNA damage and mis-repair assumptions, while the former suggests a supra-linear dose response occurs which increases the risk at low doses compared to the TE model. The NTE model is supported by many mechanistic studies using micro-beams to direct radiation to target cells, medium transfer from irradiated to unirradiated cells, and inhibitors of reactive oxygen species, gap junctions and signalling pathways. The totality of these studies provides important evidence for NTEs, which should be prioritized in light of the scarcity of both human epidemiology and animal carcinogenesis studies for high LET radiation at the low doses and dose-rates that occur in space.

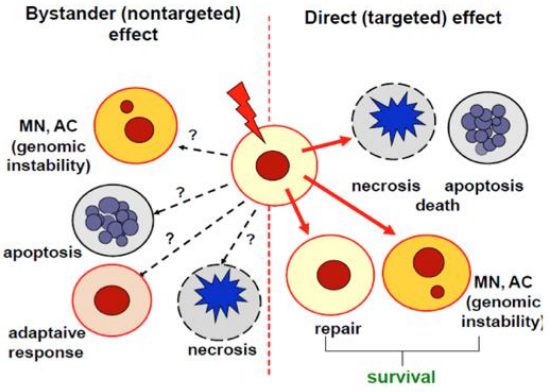

Fig. 1. The IR Bystander (Non-Targeted) Effect and Direct (Targeted) Effect (credit: Vidal M., IACSUT, Akademicka, Poland)

Figure 1 illustrates the cellular effects caused by the direct exposure of cells to ionization radiation, and the BEs resulting from the operation of particle signals secreted by irradiated cells.

BEs in neighbour cells of cells directly hit by radiation tracks and genomic instability in the progeny of irradiated cells, challenge traditional radiation protection paradigms on Earth. It is thus of interest to understand how NTE could impact our understanding of cancer risks from GCRs, which are comprised of high-energy protons and heavy ions.

1.4 Dose-Effect Relationship and dose Effects Models

The *Dose-Effect Relationship (DER)* is the relationship between the dose of IR producing cancer and the severity of their effect on exposed cells or organs. It is an increase of the risk with dose to a maximum effect followed by a decreasing of risk (levelling-off of the risk) with dose to a minimum. Therefore, dose-effect relationships describe the observed damages to normal tissues or cancer induction during and after space flights. They are developed for the various dose ranges and radiation qualities characterizing the actual and the forecast space missions [International Space Station (ISS) and solar system exploration]. Were as the *Dose-Effect Model* is reliable mathematical models of dose-effect relationship that describe the correlation between the exposition to IR and the possible damages to the organs at risk. It considers the probability to toxicity to the IR and the probability of cell survival after irradiation. The dose-effect models are one of the relevant topics of space radiobiology. Their knowledge is crucial for optimizing radioprotection strategies (e.g., spaceship and lunar space station-shielding and lunar/Mars village design), the risk assessment of the health hazard related to human space exploration, and reducing damages induced to astronauts from galactic cosmic radiation. [9, 37-39].

Crucial point is to predict the toxicity of the space radiation expected for the astronauts/space workers and the creation of reliable mathematical models that describe the correlation between the exposition to IR and the possible damages to the organs at risk.

It is important to implement a platform including the more reliable dose-effect models for space radiation, we developed an ad hoc software in R-script language.

2. Material and methods

The work reported, the calculation of the Tumor Prevalence (TP) of the γ-ray and CPs (high energy proton ions and heavy ions) including the more reliable dose-effect models for space radiation.

Prevalence is the number of people/cells with a specific disease or condition in each population at a specific time. This measure includes both newly diagnosed and pre-existing cases of the disease.

TP is described by a Hazard function, H, which is dependent on radiation type for γ-rays while for charged particles is dependent on the charge number (Z), kinetic energy (E) and fluence (F).

$$TP = 1 - e^{-H(Z,\ E,F)} \tag{1}$$

In experiments [13-17], the HG tumor prevalence was expressed as the number of animals with tumor(s) divided by the total number of animals in the experimental group. In these publications, although there are two HG per mouse, one near each eye, however the number of animals with HG tumors was used as the numerator for the prevalence calculation.

In the work reported here we considered a track structure model of TP with TE and NTE assumptions, which is used to describe the Harderian gland experiment and extrapolate the results to make predictions for low dose and dose-rate GCR exposures. Results are compared to a recently published study using a LET dependent model fit to the same data [16,17], and then applied to predictions of GCR exposures. In the remainder of this paper, we first discuss a Hazard function for TP using a track structure model consistent with either TE or NTE models. In the results section we first compare the model to experimental data for protons and heavy ions. We then use models of space radiation environments and radiation transport to compare the track structure model to the LET dependent model for nominal spacecraft shielding, and of the TE to NTE predictions.

For γ-rays we used the following form for the Hazard function:

$$H_\gamma = H_0 + \left[\alpha_\gamma D + \beta_\gamma D^2\right] S(D) \tag{2}$$

In Equation (2), H0 represents the background prevalence when animals are sacrificed, α_γ and β_γ are the linear and quadratic with dose induction terms, and S(D) the cell survival probability.

For charged particles, we considered a track structure model that extrapolates to low doses (or low fluence) to the functional form used in the NASA cancer risk assessment model [1, 30], which is consistent with a TE model that assumed a linear dose response at low doses. The Hazard function for particles is modified by the cell survival probability, *S*, and in the TE model given by:

$$H_{TE}(Z,\ E,\ F) = H_0 + \ [\ \Sigma F + \beta D^2]S \quad (3)$$

We also considered a NTE model, which assumed a non-linear type of response in addition to the linear dose term at low doses. We used these models to make a global fit to the data [22-24]. The Hazard function for particles is modified by the cell survival probability, *S*, and in the NTE model given by:

$$H_{NTE}(Z,\ E,\ F) = H_0 + \ [\Sigma F + \beta D^2 + \ \eta]S \quad (4)$$

The η function represents the NTE contribution, which is parameterized as a function of the particle LET (L).

$$\eta = \eta_0 L e^{-\eta_1 L}[1\ -\ e^{-N_{Bys}}] \quad (5)$$

Where, L is the LET of the particle,
N_{Bys} = *F*luence $* A_{Bys}$ and
A_{Bys} the number of bystander cells surrounding a cell traversed directly from a HZE particle that receive an oncogenic signal.

Following the parametric track structure model described in prior reports [1, 23] we write an effective pseudo-biological action cross section for TE per particle as:

$$\Sigma(Z,E) = \Sigma_0 P(Z,E) + \frac{\alpha_\gamma L}{6.24}[1 - P(Z,E)] \quad (6)$$

$$P(Z,\ E) = [1 - e^{\left(-\frac{Z^{*2}}{k v_c^2}\right)}]^m \quad (7)$$

where Z* is the effective charge number of the particle, and v_c is the particle velocity relative to the velocity of light. The constant α_γ is the linear regression coefficient for acute doses of γ-rays for the same endpoint.

In Equations (3) and (4), we considered a global fit to the value of β however using the adjustment:

$$\beta(Z,E) = \beta_\gamma[1 - P(Z,E)] \quad (8)$$

Equation (8) allows the influence of the dose-squared term to smoothly diminish with increasing ionization density or LET similar to the result found in the track structure model which can be described using either multi-target, multi-hit, or α-β models as described by Katz28. These different approaches led to modest changes in fits, and we used Equation (8) in the results below.

Cell Survival Function (CSP). Dimajo et al. [34] performed ex-vivo analysis of the dose response for cell survival in the Harderian gland after X–ray irradiation using male CBA/Cne mice. In their report, cell survival was well fit using the multi-target model with extrapolation number, m_S, and radio-sensitivity parameter D_0 using:

$$S(D) = [1 - (1 - e^{-D/D_0})^{m_S}] \quad (9)$$

However, because of the mouse strain differences and possible differences between male and female mice, we also considered allowing D_0 and m_S to be fit to the dose response data for tumor prevalence.

We implement this function in a r-script library (see Appendix A).

We note an earlier estimate [22] of these data found m_s=3 and D_0= 2.6 Gy.

Considering the track structure model for particles27, the CSP is given by:

$$S(Z,E,F) = [1 - \left(1 - e^{-D/D_\gamma}\right)^{m_s}]e^{-(\delta_{0S}P(Z,E)F)} \quad (10)$$

Where: $D_\gamma(Z,E) = D[1 - P(Z,E)]$ and

$$P_s(Z,E) = [1 - e^{\left(-\frac{Z^{*2}}{k_s v_c^2}\right)}]^{m_s}$$

We tuned the radiobiological parameters to reproduce available experimental data.

"The scarcity of data with animal models for tissues that dominate human radiation cancer risk, including lung, colon, breast, liver and stomach, suggest that **studies of NTEs in other tissues are urgently needed** prior to long-term space missions outside the protection of the Earth's geomagnetic sphere"

2.1 Experimental Data Set

In this study, the experimental data set was taken from Alpen et. al. [22], where the experimental test system of the study was on the development of neoplasia in the HGT of the mouse (See table I and table II). Where the estimation of the initial slope of the dose-response curve for the relationship between the dose and the increase in the prevalence of the tumors in the Harderian gland, and the estimation of the dependence of this slope on the LET of the radiation.

2.1.1 Linear Energy Transfer of Particle Ions

The charged particle beams were available at the BEVALAC facility of the Lawrence Berkeley Laboratory. The dose-measuring systems and beam monitors have been described by Lyman and Howard [34] and Curtis [36]. The Latter paper provides an overview on the calculated LET values for heavy ion

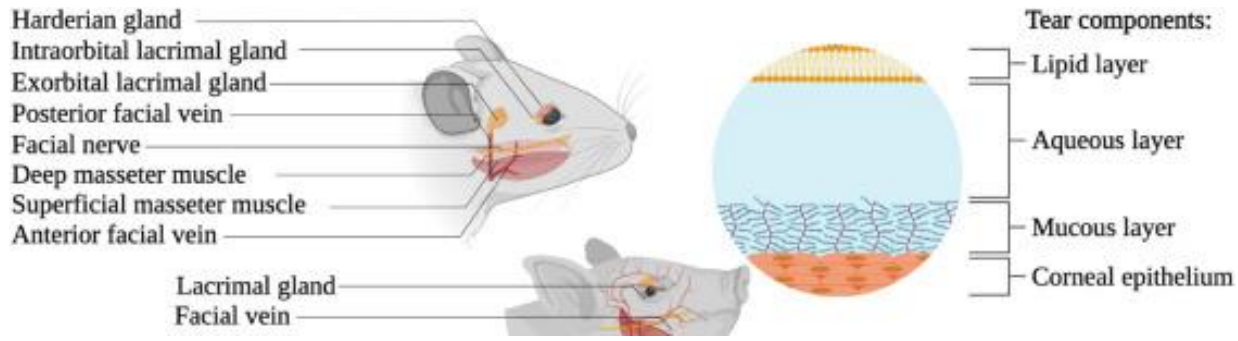

Fig. 2. Anatomy of the mouse showing Harderian Gland Tumors. (Credit: SLAS Discovery)

beams: however, we routinely used values provided by B. Ludewigt from a more recent code developed by the BEVALAC staff.

The estimates of dose averaged LET_∞ values for the various ion beams were based on the charge and residual range of the beam particles. For our considerations of fluence-based risk coefficients under Discussion, track-averaged LET values are appropriate. However, in the initial plateau region of the Bragg Ionization curve used in these studies, the track-averaged and dose-averaged LETs are essentially the same. The residue range can be measured directly using a variable water column, it can be calculated, because the particle energy at the accelerator exit window (±0.5%) and amount of material in the beam line (±1 mm) are known. The nominal energies, LET_∞ values and maximum ranges for the ions used are shown in table I.

Table I
Nominal Energies, LET_∞, [a] and Maximum Ranges in Water

Mice			
Ions	Energy (A MeV)	Entrance LET_∞ (KeV/μm)	Range in Water (cm)
Hydrogen, $^{1}_{1}H$	250	0.4	25
Helium. $^{4}_{2}He$	228	1.6	26
Neon. $^{20}_{10}Ne$	670	25	31
Iron, $^{56}_{26}Fe$	600	193	9.7
Iron, $^{56}_{26}Fe$	350	253	2.5
Niobium, $^{43}_{93}Nb$	600	464	4.8

[a] The values are for dose-averaged LET; however, at the zero absorber position in the plateau region of the Bragg curve, dose-averaged LET and track-averaged LET are essentially the same.

2.1.2 Prevalence of Harderian Gland Tumors

The mice were irradiated when they were 100 to 120 days old. The charged particle beams were collimated with a Cerrobend alloy collimator a 3 x 5 cm field for irradiation of the head and supper thorax area. The anesthetized mice were secured into individual compartments on a Lucite plate so that the Harderian gland was always positioned at the centre of the beam. One mouse at a time was aligned into the beam path by computer-controlled sample translator. A standard configuration of ionization champers were column, collimators and translator were used for all exposures [32].

A 55.5 TBq 60Co γ-ray source was used as the low-LET reference radiation. The mice were anesthetized as for the BEVALAC irradiations and secured in Lucite holder with 1.2 cm lead covering all but the head and thorax. Dose measurements were made with a Vactoreen thimble ion chamber calibration against an NIST secondary standard. Irradiation time were generally 5 to 10 min.

The second order polynomial was fitted to the data for ^{60}Co 55.5 TBq γ irradiation (Table II).

Table II
Prevalence of Harderian Gland Tumours After 60Co Gamma Irradiation

Mice				
Dose (Gy)	Number	At risk	With tumours	Prevalence[a] (%)
0	198	155	4	2.6 ± 2.5
0.4	292	229	11	4.8 ± 2.7
0.8	278	161	15	9.3 ± 4.5
1.6	244	117	16	13.7 ± 6.2
3.2	181	115	37	32.2 ± 8.5
7.0	90	52	24	46.2 ± 13.6

[a] ±95% CI

The higher doses, which show significant saturation effect, are omitted from the regression analysis, in this case the 7.0 Gy dose. The fitting regression equation for the range of doses used in the fitting is shown in fig. 3. The fit suggests that the second-order polynomial model is good description of the relationship between dose and TP. The value R2 for the fit is 0.99 indicating a very small residual not accounted for in the second order fit.

3. Theory and calculation

3.1 Effective Pseudo-Biological Action Cross Section single column and find the credit for the HGT

Using the experimental data of gamma irradiation, we calculate the αγ, βγ induction term, here the parameter αγ is used in equation (6) to calculate the Effective Pseudo-Biological Action Cross Section or Eta ($\Sigma(Z, E)$) for hydrogen ions (proton ions) of 250A MeV and 0.4 keV/μm of LET.

In the figure 3 below the blue line indicates the second order polynomial fitted curve to the Hydrogen ions data points taken from Alpen et. al., and the green line is the linear fit to the same data points.

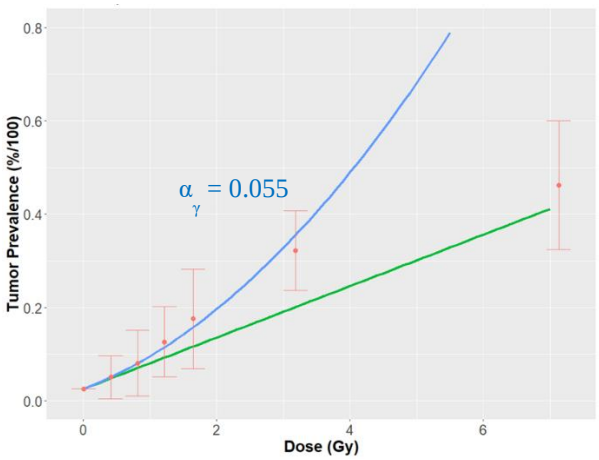

Fig. 3. Tumour Prevalence vs Dose for for 60Co 55.5 TBq γ-ray irradiation. The red points are the experimental data points of hydrogen ions taken from Alpen .et .al [22], the error bars indicate the maximum and minimum deviation of the prevalence of the data point, the blue curve indicates the second order polynomial fit to the first three data points, and the green curve is the linear fit and to the data points.

$$\Sigma(1,\ 250) =$$

$$\Sigma_0 P(Z,\ E) + \frac{0.55*0.4}{6.24}[1 - P(1,\ 250)] \qquad (11)$$

$$P(1,\ 250) = [1 - e^{\left(-\frac{Z^{*2}}{k v_c^2}\right)}]^3 \qquad (12)$$

Where:

- Σ_0 and k are parameters of his cellular track structure model
- α_γ is the linear regression coefficient for acute doses of γ-rays for the same endpoint
- Z^* is the effective charge number of the particle,
- *Vc* is the particle velocity relative to the velocity of light
- m is the number of targets in a single cell

3.2 Linear and Quadratic regression coefficient (α_H, β_H) Calculation

Using the experimental data of 250A MeV Hydrogen irradiation we calculate the α_H, β_H induction term.

Table III
Prevalence of Harderian Gland Tumours after Irradiation with Proton ions

Mice				
Dose (Gy)	Number	At risk	With tumours	Prevalence[a]
0	198	155	4	2.6 ± 2.5
0.4	47	44	43	9.3 ± 6.1
0.8	42	41	8	19.5 ± 12.1
1.6	48	43	13	30.2 ± 13.7
3.2	28	24	7	29.2 ± 18.2

[a] ±95% CI

The quadratic regression coefficient is used equations (3) and (4) in the calculation of hazard functions of TE and NTE. In the figure 4 below the blue curve indicates the second order polynomial fitted curve to the first three proton data points taken from Alpen et. al., and the green line is the linear fit to the same data points.

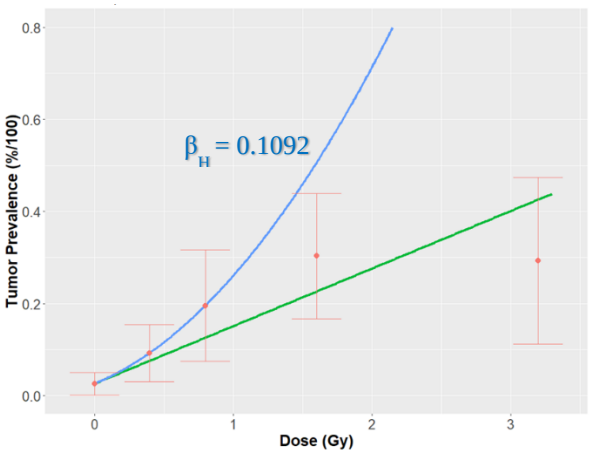

Fig. 4. Tumour Prevalence vs Dose for hydrogen ions (Proton) iradiation. The red points are the experimental data points of hydrogen ions taken from Alpen .et .al [22], the error bars indicate the maximum and minimum deviation of the data point, the blue curve indicates the second order polynomial fit to the first three data points, and the green curve is the linear fit and to the data points.

$$H_{NTE}(1,\ 250,\ F) =$$

$$0.026 + [\Sigma(1{,}250) * F + 0.1092 * D^2 + \eta_H] * S \qquad (13)$$

$$\eta_H = 0.00048 * 0.4e^{-0.00281*0.4}[1 - e^{-216*F}] \quad (14)$$

Where, β_H is the quadratic coefficient with dose induction terms, irradiation for hydrogen

For the cell survival probability is used the target theory n-target N-hit model (nTNH) with n =3, N = 1

4. Results: Target Effect (TE) vs Non-Target Effect (NTE) for Proton

4.1 TE and NTE Models

Calculation of the TE and NTE TP models showing for Proton 250A MeV there is no relevant differences in the Tumour Prevalence versus dose as expected. In the figure 5 and figure 6 below all the components of hazard function are indicated as: the Survival Fraction Probability by blue curve, the βD^2 is by red curve, ΣF component is light green curve, and the η component is by indigo curve. The overlapped dotted violet and green indicates the TE and NTE track models obtained by fit the proton data points taken from Alpen et. al. [22].

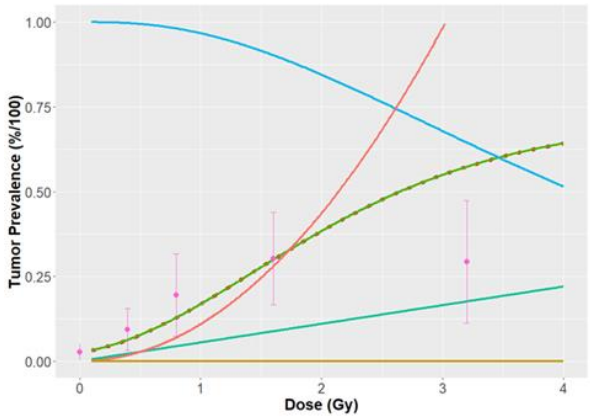

Fig. 5. Tumour Prevalence vs Dose TE and NTE model for proton ions irradiation. The red points are the experimental data points of proton ions taken from Alpen .et .al [22], the error bars indicate the maximum and minimum deviation of the data point. The blue curve is the CSP model, the red curve is βD^2 component, light green curve is ΣF component, and the indigo curve is η component of the hazard function. The overlapped dot violet and green curves indicate the TE and NTE track models respectively.

The shape of the tumor response curve found in the NTE model is shallow non-linear dose responses curve. It has important implications for space travel because would alter how mission design factors such as duration and radiation shielding are analyzed for radiation protection purposes.

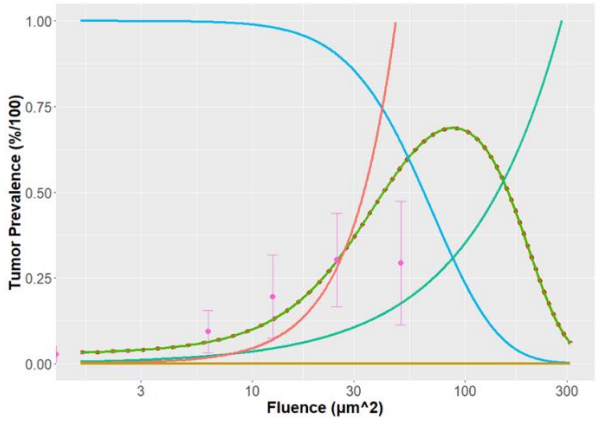

Fig. 6. Tumour Prevalence vs Fluence TE and NTE model for proton ions irradiation. The red points are the experimental data points of proton ions taken from Alpen .et .al [22], the error bars indicate the maximum and minimum deviation of the data point. The blue curve is the CSP model, the red curve is βD^2 component, light green curve is ΣF component, and the indigo curve is η component of the hazard function. The overlapped dot violet and green curves indicate the TE and NTE track models respectively.

4.2 A Tool for NTE calculation

In this study we have developed reliable mathematical models, Dose-Effect Models (DEMs) for the calculation of TP of high energetic proton ions and heavy ions in terms of hazard function of the TE and NTE models as a tool. In the future, it is the possibly to use this tool automatically in the calculate the NTE in different models and different exposure scenario including the data taken from AMS and other astroparticle experiments. The software comprises a "main program" and several libraries for a total of >10K lines of code for gamma 55.5TBq Co60 and different charged particles such as high energetic 250A MeV proton Ions (Hydrogen Ions ($^1_1$H)), 228A MeV Helium Ions ($^4_2$He), 670A MeV Neon Ions ($^{20}_{10}$Ne), 260A MeV Silicon Ions ($^{14}_{28}$Si), 1000A MeV Titanium Ions ($^{22}_{48}$Ti), (540A MeV, 600A MeV and 350A MeV) Iron Ions ($^{56}_{26}$Fe), 600A MeV Niobium Ions ($^{93}_{43}$Nb), and 593A MeV Lantanio ($^{57}_{139}$La).

4.2.1 Inputs

Some important parameters used as input are the LET, the kinetic energy, atomic number of the particle, the dose interval, the background Tumour Prevalence (H_0) and the selection of most relevant Cell Survival Probability model.

4.2.2 Output

The fluence (F) of the particles, linear and quadratic regression coefficient (α and β), the η function, the pseudo-biological action cross section ($\boldsymbol{\Sigma}$), the hazard

function for TE and NTE model, the TP are all the output of the calculation. Finally, the plots of Dose vs Tumour Prevalence (%) and the plot of particle Fluence vs Tumour Prevalence (%) are the results of the model.

5. Discussion and Conclusion

We developed an ad hoc software in R-script language for TP risk calculation including the more reliable dose-effect models for space radiation

An r-script library with different Cell Survival Probability models was developed to be used in the calculation of hazard functions of TP.

Using the software and the experimental data set of HGT we tune all the parameter for the TP model for protons and we show that there are no substantial differences between the TE and NTE as expected. (For hydrogen ions, the NTE models predict same tumor prevalence at low doses compared to the TE model when a global fit to the Alpen et al. [22] data is made).

In the future, we extend the analysis to heavy ions, and we will use the data collected from the AMS02 detector and other astroparticle experiments see Fig. 7 to increase the modelling accuracy and risk prediction.

Acknowledgements

We gratefully acknowledge the strong support from the AMS collaboration, from the INFN Scientific Committee 2 (CSN2) and from the Italian Space Agency (ASI) within the agreement ASI-INFN n. 2019-19-HH.0.

Appendix A *HGT_CPS Library for Cells Survival Probability models to use in IR exposure Risks Assessment in Space*

Using the R-Studio IDE, we developed in r-script library including all the relevant Cell Survival Probability (CSP) models both for the gamma-ray and charged particles relevant for space radiation and, to be used in the calculation of TP,

In this CSP models the absorbed dose, the number of target (n) and the number hit (N), the effective charge number of the particle (Z^*), the particle velocity relative to the velocity of light (V_c), and the number of targets in a single cell (m) are the important parameters as input were as Cell Survival Probability (CSP) model is the output of the calculation.

linear and quadratic regression coefficient (α and β),

The implemented CSP models in the library are:

I. Target Theory n-target N-hit model (nTNH)
   Two special cases of nTNH including:
   a. Theory single Target single hit model (sTSH)
   b. Theory single Target N-hit model (sTNH)

$$S(D) = 1 - (1 - B)^n, B = e^{\frac{-D}{D_0}}[1 + \sum_2^N \frac{\left(D/D_0\right)^{N-1}}{(N-1)!}] \quad (15)$$

II. Theory Linear Quadratic Model (LQ)

$$S(D) = e^{-\alpha D - \beta D^2} \quad (16)$$

III. Linear Quadratic Model modified by hyper-radiosensitivity (HRS) effect.

$$S(D) = exp\{-\alpha\left(1 + \left(\frac{\alpha_s}{\alpha} - 1\right)e^{\frac{-D}{D_0}}\right)D - \beta D^2\} \quad (17)$$

IV. Theory Linear Quadratic Cubic Model (LQC) for high dose.

$$S(D) = e^{-\alpha D - \beta D^2 - \gamma D^3} \quad (18)$$

V. Sublesion Theory Repair – misRepair Model (S-RMR)

$$S(D) = e^{-aD}[1 + (\frac{aD(1-e^{(-\lambda T)})}{\varepsilon})]^{\varepsilon\phi} \quad (19)$$

VI. Sub-lesion Theory Lethal – potentially lethal Model (S-LPL)

$$S(D) = e^{-(n_L - n_{PL})D}[1 + \frac{n_{PL}D}{\epsilon}(1 - e^{-\epsilon_{PL}t_r})]^{\epsilon} \quad (20)$$

VII. Sublesion Theory Saturable Repair Model (S-SR)

$$S(D) = e^{-\frac{n_0 - C_0}{1 - \frac{C_0}{n_0}e^{kT(C_0 - n_0)}}} \quad (21)$$

References

[1] F. A. Cucinotta, M. Alp, B. Rowedder, & M. Kim, Y. Safe days in space with acceptable uncertainty from space radiation exposure. Life Sciences in Space Research 5, (2015) 54–69, doi: 10.1016/j.lssr.2015.04.002

[2] F. A. Cucinotta, M. Alp, F. M. Sulzman, & M. Wang, Space radiation risks to the central nervous system. Life Sciences in Space Research 2, (2014) 54–69, doi: 10.1016/j.lssr.2014.06.003

[3] NCRP. Information needed to make radiation protection recommendations for space missions beyond Low-Earth orbit. National Council on Radiation Protection and Measurements, 2006, Report No. 153: Bethesda MD

[4] A. Bartoloni, G. Della Gala, A.N. Guracho G. Paolani, M. Santoro L. Strigari, S. Strolin. High energy Physics Astro Particle Experiments to Improve the Radiation Health Risk Assessment for Humans in Space Missions, in Proceedings of the European Physical Society Conference on High Energy Physics EPS-HEP2021, vol. 398, p.106, DOI:10.22323/1.398.0106, (2022).

[5] F. A. Cucinotta, *et al*. Space radiation and cataracts in astronauts. *Radiation Research* **156**, (2001) 460–466, doi: 10.1667/0033-7587.

[6] L. T. Chylack, *et al*. NASCA Report 1: Cross-sectional study of relationship of exposure to space radiation and risk of lens opacity. *Radiation Research* **172**, (2009) 10–20, doi: 10.1667/RR1580.1

[7] F. A. Cucinotta, N. Hamada, & M. P. Little, Commentary — No evidence for an increase in circulatory disease mortality in astronauts following space radiation exposures. *Life Sciences in Space Research* **10**, (2016) 53–56, doi: 10.1016/j.lssr.2016.08.002

[8] M. P. Little, *et al*. Systematic review, and meta-analysis of circulatory disease from exposure to low-level ionizing radiation and estimates of potential population mortality risks. *Environmental Health Perspectives* **120**, (2012) 1503–1511, doi:10.1289/ehp.1204982

[9] L. Strigari, S. Strolin, A. G. Morganti and A. Bartoloni, DEMs for space radiobiology: an overview on dose effect relationships, to be published on Frontiers in Public Health- Radiation and Health, DOI: 10.3389/fpubh.2021.733337, (2021)

[10] NCRP. Recommendations of dose limits for LEO. National Council on Radiation Protection and Measurements, NCRP Report 132: Bethesda MD (2000).

[11] F. A. Cucinotta, M. Y. Kim, & L. Chappell, Space radiation cancer risk projections and uncertainties-2012. NASA TP 2013–217375.

[12] T.C. Evants, Effect of small daily doses of fast neutrons in mice. *Radiology* **50**, (1948) 811 – 834.

[13] A. C. Upton, M L. Randolph, and L. W. Conklin, Late effects of fast neutrons and gamma-ray in mice as influenced by the dose rate of irradiation: Induction of neoplasia. *Radiat*. Res. **41**, (1970) 467 – 491.

[14] R. L. Ullrich, Tumour Induction in BALAN/c mice after fractionated or protracted exposures to fission spectrum neutrons. *Radiat*. Res. **97**, (1984) 587 – 597.

[15] J. F. Thomson, F. S. Williamson, D. Grahn, and E. J. Ainsworth, Life shortening in mice exposed to fission neutrons and γ-ray. I. Single and short-term fractionated exposures. *Radiat*. Res. **88**, (1981), 559 – 572.

[16] F.A. Cucinotta, E. Cacao, Non-Targeted Effects Models Predict Significantly Higher Mars Mission Cancer Risk than Targeted Effects Models. *Sci Rep* **7**, (2017) 1832 https://doi.org/10.1038/s41598-017-02087-3

[17] W. K. Sinclair, Fifty years of neutronsin biology and medicine. The comparative effectives of neutrons in biological systems. In *Eighth Symposium on Microdosimetry* (J. Booz and H. G. Ebert, Eds.), Commission of the European Communities, Harwood, London, 1982, pp. 1 – 37.

[18] C. W. Mays and H. Spiess, Bone sarcomas in patients give radium-224. In *Radiation Carcinognesis: Epidemology and Biological Significance* (J. D. Boice, Jr., and J. F. Fraumeni. Jr., Eds.), Raven Press, New York, 1984, pp. 241 – 252.

[19] R. J. M. Fry. P. Powers-Risius, E. L. Alpen, and E. J. Ainsworth, High-LET radiation carcinogenesis. *Radiat*. Res. **104**, (1985) S188 – S195.

[20] F. A. Cucinotta, A new approach to reduce uncertainties in space radiation cancer risk predictions. (2015) PLoS One e120717.

[21] R. J. M. Fry, P. Powers-Risius, E. L. Alpen, & E. J. Ainsworth, High LET radiation carcinogenesis. Radiation Research 104, (1985) S188–S195, doi:10.2307/3576646.

[22] E. L. Alpen, P. Powers-Risius, S. B. Curtis & R. DeGuzman, Tumorigenic potential of high-Z, high-LET charged particle radiations. Radiation Research 88, (1993) 132–143, doi:10.2307/3578551.

[23] E. L. Alpen, et al. Fluence-based RBE for charged particle carcinogenesis in mouse Harderian gland.

Advances in Space Research 14, (1994) 573–581, doi:10.1016/0273-1177(94)90512-6).

[24] P. Y. Chang, et al. Harderian gland tumorigenesis: low-dose- and LET-Response. Radiation Research 185, (2016) 448–459, doi:10.1667/RR14335.1

[25] W. F. Morgan, Non-targeted and delayed effects of exposure to ionizing radiation. I. Radiation-induced genomic instability and BEs in vitro. Radiation Research 159, (2003). 567–580, doi:10.1667/0033-7587.

[26] C. A. Maxwell, et al. Targeted and nontargeted effects of ionizing radiation that impact genomic instability. Cancer Research 68, (2008) 8304–8311, doi: 10.1158/0008-5472.CAN-08-1212.

[27] M. Kadhim, et al. non-Targeted effects of ionizing radiation- implications for low dose risk. Mutation Research 752, (2013) 84–98, doi: 10.1016/j.mrrev.2012.12.001.

[28] F. A. Cucinotta & L. J. Chappell, Non-targeted effects, and the dose response for heavy ion tumour induction. Mutation Research 687, (2010) 49–53, doi: 10.1016/j.mrfmmm.2010.01.012.

[29] M. Hada, L. J. Chappell, M. Wang, K. A. George & F. A. Cucinotta, On the induction of chromosomal aberrations at fluence of less than one HZE particle per cell nucleus. Radiation Research 182, (2014) 368–379, doi:10.1667/RR13721.1

[30] E. Cacao, M. Hada, P. B. Saganti, K. A. George & F. A. Cucinotta, Relative biological effectiveness of HZE particles for chromosomal aberrations and other surrogate cancer risk endpoints. (2016) PLoS One 11, e0153998, doi: 10.1371/journal.pone.0153998.

[31] F. A. Cucinotta & J. W. Wilson, Initiation-promotion model for tumour prevalence from high energy and charge radiation. Physics in Medicine and Biology 39, (1994) 1811–1831, doi:10.1088/0031-9155/39/11/003.

[32] F. A. Cucinotta & J. W. Wilson, Initiation-promotion model of tumour prevalence in mice from space radiation exposure. Radiation and Environmental Biophysics 34, (1995) 145–149, doi: 10.1007/BF01211540.

[33] F. A. Cucinotta, H. Nikjoo & D. T. Goodhead, Comment on the effects of delta-rays on the number of particle-track transversals per cell in laboratory and space exposures. Radiation Research 150, (1998).115–119, doi: 10.2307/3579651

[34] V. Di Majo, et al., Dose-response relationship of radiation-induced HGTs and myeloid leukemia of the the CBA/CNE mouse. Journal of the National Cancer Institute 76, (1986) 955–963.

[35] J. T. Lyman and J. Howard, Dosimetry and instrumentation for helium and heavy ions. *Int. J. Radiat. Oncol. Biol. Phys.* **3**, (1977), 81 – 85

[36] S. B. Curtis, Calculated LET distributions of heavy ion beams. *Int. J. Radiat. Oncol. Biol. Phys.* **3**, (1977) 87 – 91.

[37] A. Bartoloni, S. Strolin, L. Strigari, 2020 Virtual IEEE Nuclear Science Symposium and Medical Imaging Conference http://wiki.infn.iroma1/experiments/ams2/ieee-nss-mic_bartoloni5.pdf (accessed 30.10.2022).

[38] A. Bartoloni, L. Strigari, AMS02 e radiobiologia nello spazio, Annual Conference of the Italian Physical Society (SIF) L'Aquila 27/09/2019, wiki.infn.it/_media/strutture/roma1/experiments/ams2/ams_sprb_sif_2209_breve_eng.pdf (accessed 31.08.22)

[39] A. Bartoloni, L. Strigari, Can high energy particle detectors be used for improving risk models in space radiobiology? in proceedings of the Global Space Exploration Conference 2021 (GLEX2021) Jun 2021.